JBC ARTICLE

The *Trypanosoma brucei Tb*Hrg protein is a heme transporter involved in the regulation of stage-specific morphological transitions

Received for publication, October 12, 2016, and in revised form, February 21, 2017 Published, Papers in Press, February 23, 2017, DOI 10.1074/jbc.M116.762997

Eva Horáková[‡1], Piya Changmai[‡1,2], Marie Vancová[‡§], Roman Sobotka[§¶], Jan Van Den Abbeele[‖], Benoit Vanhollebeke[**], and Julius Lukeš[‡§‡‡3]

From the [‡]Institute of Parasitology, Biology Center, Czech Academy of Sciences, 37005 České Budějovice (Budweis), Czech Republic, [§]Faculty of Sciences, University of South Bohemia, 37005 České Budějovice (Budweis), Czech Republic, [¶]Institute of Microbiology, Czech Academy of Sciences, 37981 Třeboň, Czech Republic, [‖]Department of Biomedical Sciences, Unit of Veterinary Protozoology, Institute of Tropical Medicine, B2000 Antwerp, Belgium, [**]Institut de Biologie et de Médecine Moléculaires, Université Libre de Bruxelles, B6041 Gosselies, Belgium, and [‡‡]Canadian Institute for Advanced Research, Toronto, Ontario M5G 1Z8, Canada

Edited by Joseph Jez

The human parasite *Trypanosoma brucei* does not synthesize heme *de novo* and instead relies entirely on heme supplied by its vertebrate host or its insect vector, the tsetse fly. In the host bloodstream *T. brucei* scavenges heme via haptoglobin-hemoglobin (HpHb) receptor-mediated endocytosis occurring in the flagellar pocket. However, in the procyclic developmental stage, in which *T. brucei* is confined to the tsetse fly midgut, this receptor is apparently not expressed, suggesting that *T. brucei* takes up heme by a different, unknown route. To define this alternative route, we functionally characterized heme transporter *Tb*Hrg in the procyclic stage. RNAi-induced down-regulation of *Tb*Hrg in heme-limited culture conditions resulted in slower proliferation, decreased cellular heme, and marked changes in cellular morphology so that the cells resemble mesocyclic trypomastigotes. Nevertheless, the *Tb*Hrg KO developed normally in the tsetse flies at rates comparable with wild-type cells. *T. brucei* cells overexpressing *Tb*Hrg displayed up-regulation of the early procyclin GPEET and down-regulation of the late procyclin EP1, two proteins coating the *T. brucei* surface in the procyclic stage. Light microscopy of immunostained *Tb*Hrg indicated localization to the flagellar membrane, and scanning electron microscopy revealed more intense *Tb*Hrg accumulation toward the flagellar pocket. Based on these findings, we postulate that *T. brucei* senses heme levels via the flagellar *Tb*Hrg protein. Heme deprivation in the tsetse fly anterior midgut might represent an environmental stimulus involved in the transformation of this important human parasite, possibly through metabolic remodeling.

Heme, an iron-containing porphyrin, is a prosthetic group involved in numerous key cellular processes in the majority of extant organisms (1). Due to its capacity to transfer electrons and bind diatomic gases, heme is implicated in oxidative metabolism such as electron transport-dependent oxidative phosphorylation, oxidative stress response, oxygen transport, sensing, and detoxification. It is also used as a signaling molecule in many aerobic organisms (2). In heterotrophic eukaryotes, the first step of heme biosynthesis involves the condensation of glycine with succinyl-CoA, whereas photosynthetic eukaryotes initiate its synthesis from glutamate bound to $tRNA^{GLU}$. However, all seven subsequent steps of heme biosynthesis are performed by enzymes highly conserved in all three domains of life (3, 4).

In contrast to organisms capable of synthesizing heme, trypanosomes and related flagellates belong to a small group of eukaryotes that do not synthesize heme *de novo* and totally rely on external heme (5, 6). As heme auxotrophs, they acquire this prosthetic group from their invertebrate vector or their vertebrate host. Interestingly, there seems to be a fundamental difference in a way distinct life cycle stages of trypanosomes acquire heme. The bloodstream stage (BS)[4] of *T. brucei*, which is covered by a hypervariable variant surface glycoprotein (VSG) (7), proliferates in blood with haptoglobin-hemoglobin (HpHb) complexes being the major source of extracellular circulating heme (8). The BS flagellates obtain heme via a specific HpHb receptor localized in the flagellar pocket (9). However, in the procyclic stage (PC), which is confined to the midgut of the tsetse fly vector and has its surface covered with two coat proteins, GPEET and EP procyclins (10), the HpHb receptor appears not to be expressed (9, 11). Nevertheless, due to an active respiration chain and a corresponding requirement for cytochromes (12, 13), the PC cells are likely to require more heme than the BS trypanosomes. Moreover, in the posterior midgut (PM), PCs transiently face a high amount of free heme as a consequence of large quantities of ingested vertebrate blood (14). From there, the parasites expand in the ecto-

This work was supported by the Czech Grant Agency (16-18699S; to J. L.) and by the Interuniversity Attraction Poles Programme, Belgian Science Policy (to J. V. D. A. and B. V.). The authors declare that they have no conflicts of interest with the contents of this article.

[1] Both authors contributed equally to this work.

[2] Present address: Life Science Research Centre, Faculty of Science, University of Ostrava, 701 03 Ostrava, Czech Republic.

[3] Recipient of COST action CA15133. To whom correspondence should be addressed: Institute of Parasitology, Branišovská 31, 37005 České Budějovice, Czech Republic. Tel.: 420-38-777-5481; Fax: 420-38-531-0388; E-mail: jula@paru.cas.cz

[4] The abbreviations used are: BS, bloodstream stage; HpHb, haptoglobin-hemoglobin; HpHbR, HpHb receptor; PC, procyclic stage; PM, posterior midgut; AM, anterior midgut; SG, salivary gland; HRG, heme-response gene; Lhr1, *Leishmania* heme response 1; *Tb*Hrg, *T. brucei* heme-responsive gene; TMD, transmembrane domains; qRT, quantitative real-time; ns, not significant; tet, tetracycline.

peritrophic space upward to the anterior midgut (AM) accompanied by a progressive elongation of the parasites, the mesocyclic trypomastigotes. Some of these will enter the proventriculus (PV) lumen and undergo a complex differentiation into epimastigotes, which have typical anterior kinetoplast and BARP surface coat. Trypanosomes re-enter the gut lumen and migrate to the salivary glands (SG) to finish the differentiation by forming infectious metacyclic trypomastigotes (15, 16). Overall, tsetse fly digestive tract is a highly dynamic and harsh environment, where uptake, sequestration, and utilization of heme have to be tightly regulated (17).

Several paralogs of membrane-bound transporters of heme were first identified in the free-living roundworm *Caenorhabditis elegans* and named HRG (heme-response genes) (18, 19). In contrast, mammals have a single gene that is only ~20% identical to the *C. elegans* homologues (20). Previous studies have demonstrated that both roundworm and human HRG-1 bind and transport heme and that the knockdown of Hrg-1 in embryos of the zebrafish *Danio rerio* results in severe anemia, which is fully rescued by the *C. elegans* Hrg-1 homologue (18). Furthermore, the HRG genes were shown to be dramatically up-regulated (up to 200-fold) in response to heme deficiency, and their depletion resulted in aberrant cytochrome *c* distribution that was partially restored by heme supplementation (21). A single homolog of the *C. elegans* Hrg-4 gene was identified also in the genome of *Leishmania amazonensis* (Lhr1, *Leishmania* heme response 1) and in other trypanosomatids, including *Trypanosoma brucei* (22) and *Trypanosoma cruzi* (23). Notably, viable parasites with both Lhr1 alleles disrupted could not be obtained, suggesting that this gene is essential for the survival of *L. amazonensis*. Heme deprivation in these protists increased the amount of Lhr1 mRNA 4-fold, which to a limited extent mimics the situation in *C. elegans* (22). Several unique amino acids were identified to be critical for the function of Lhr1, as their mutations affected transport of heme across cellular membranes and consequently the virulence of *L. amazonensis* (24). Recently, based on RNAi evidence, *Tb*Hrg was reported to be essential in BS of *T. brucei* and was characterized as a lysosomal transporter responsible for heme salvage from hemoglobin, downstream of HpHb receptor (HpHbR)-mediated import (25).

Here we studied the function of *Tb*Hrg transporter in PC of *T. brucei*. We show that the *Tb*Hrg protein mediates heme import into the PC trypanosomes and seems to be the sole candidate for such a function in the tsetse fly. Interestingly, *Tb*Hrg is also localized in the flagellar membrane, and its overexpression coincides with remodeling of the cell surface. Moreover, expression of the *Tb*Hrg gene was observed to be at the highest level in PC harvested from the tsetse fly posterior midgut. Based on these results, we suggest that in the tsetse fly vector this transporter is involved in the regulation of the important switch from the PC into the mesocyclic trypomastigotes, perhaps via heme availability and downstream metabolic remodeling.

Results

Characterization of heme transporter in T. brucei

Based on the results of a Blast search, using *L. amazonensis* Lhr1 as a query, Tb927.8.6010 was identified as a candidate for the putative heme transporter in *T. brucei*. It has a molecular mass of 18.1 kDa and was named *Tb*Hrg (*T. brucei* heme-responsive gene). The *Tb*Hrg protein has 26% identity and 42% similarity with *L. amazonensis* Lhr1. Amino acid sequence analysis by MINNOU revealed four predicted transmembrane domains (TMD) similarly to *Leishmania* Lhr1 and Hrg-4 from *C. elegans* (Fig. 1). Even though *Tb*Hrg lacks the histidine residue between TMD3 and TMD4, conserved in Lhr1 and Hrg-4, it contains another conserved histidine in TMD2 (Fig. 1) that is essential for heme transportation in Hrg-1 from *C. elegans* as well as in human HRG-1 (26). Notably, *Tb*Hrg was found to be phosphorylated on serine 147 (27), the amino acid present also in human HRG-1 but not in its Hrg-4 or Lhr1 homologues (Fig. 1).

TbHrg is differentially expressed during the T. brucei life cycle

The expression profile of *Tb*Hrg during differentiation was reported earlier in several high-throughput studies. *Tb*Hrg mRNA was shown to be 5-fold decreased in the BS compared with PC cells (28–30) and increased in the salivary glands (31). It is known from *C. elegans* and *L. amazonensis* (21, 22) that the transcript may be also regulated by heme availability and consequently vary in different life cycle stages.

To test this possibility in *T. brucei*, we performed qRT-PCR to monitor the expression of *Tb*Hrg in the PC and BS flagellates. The analysis showed that the level of *Tb*Hrg transcript in the BS is ~10× lower than in the PC grown in regular SDM-79 (Fig. 2*A*). We also compared the levels of *Tb*Hrg transcript in PC under three cultivation conditions with different concentrations of hemin and fetal bovine serum (FBS), which serve as a source of heme in axenic culture. Unlike in other heme auxotrophs, the level of *Tb*Hrg transcript seems not to be modulated by heme availability in PC, as under all conditions tested the expression changed only slightly (Fig. 2*A*). Next, we monitored the relative abundance of *Tb*Hrg mRNA in different *T. brucei* developmental stages within the tsetse fly vector, *i.e.* in the PC, anterior midgut (mesocyclic trypomastigotes), proventriculus/foregut (post-mesocyclic trypanosomes), and salivary glands (different stages of metacyclogenesis). The *Tb*Hrg transcript abundance in these tissues was monitored by qRT-PCR using telomerase reverse transcriptase (TERT) and double-strand break repair nuclease (MRE11) mRNAs as normalizers. The tsetse *in vivo* data (Fig. 2*B*) correlated well with the experiment done with cells under axenic culture conditions. The *Tb*Hrg transcript is expressed mainly in the PC flagellates, a life cycle stage that dwells in the tsetse PM. At a later stage of the development in the tsetse fly, *i.e.* in the AM, proventriculus (PROV) and SG, the expression level of *Tb*Hrg dropped to ~50% of the posterior PC level. The AnTAR1 BS cells showed low *Tb*Hrg expression level, with a mere 10% expression as compared with the PM-derived PC cells (Fig. 2*B*).

Down-regulation of TbHrg causes a growth defect under low heme conditions

High-throughput RNAi screen predicted abnormal cell proliferation in both PC and BS stages (32). Because the protein was already found to be essential in the BS (25), we studied function of the *Tb*Hrg in the PC cells only. For that we gener-

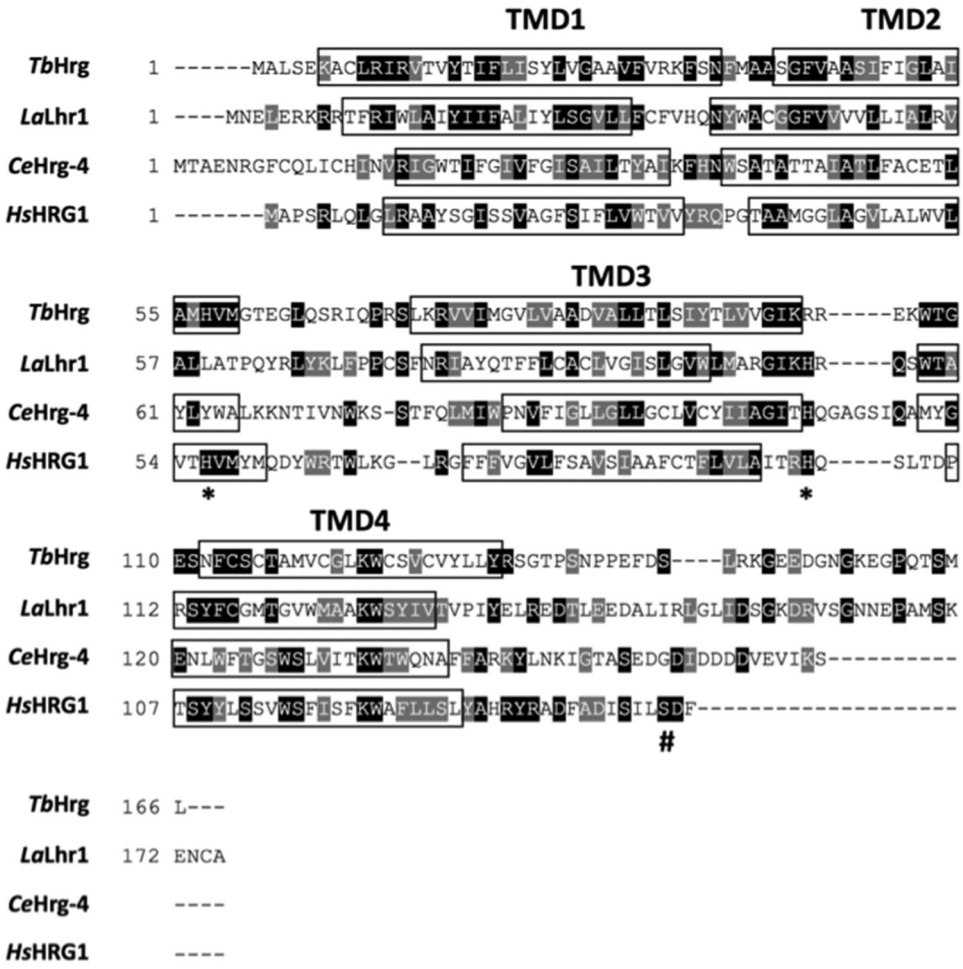

Figure 1. Multiple sequence alignment of *Tb*Hrg and its homologues. Sequence of *T. brucei* (*Tb*Hrg, TriTrypDB accession number Tb927.8.6010), *L. amazonensis* (Lhr1, Genbank™ accession number CBZ27556), *C. elegans* (Hrg-4, WormBase Gene ID WBGene00009493), and *Homo sapiens* (HRG-1, ID SLC48A1) were used in this alignment generated by ClustalW. *Boxshade* was used to highlight the identical domains. *Rectangular frames* show TMDs predicted by MINNOU in *Tb*Hrg. The TMDs in other genes are adapted from Huynh *et al.* (22). *Asterisks* indicate conserved histidine residues. # indicates phosphorylated serine at position 147 according to TritrypDB.

ated PC RNAi knockdown cell line and confirmed a substantial decrease of the *Tb*Hrg transcript by qRT-PCR. At day 4 post-RNAi induction the *Tb*Hrg mRNA level dropped by ~80% as compared with its level in the non-induced cells (Fig. 3*A*, *inset*). Based on a study from *C. elegans* (18), we decided to test cell viability under two conditions: (i) in the high heme medium, where trypanosomes are cultivated in standard SDM 79, which contains 7.5 mg/liter hemin (11.4 μM) and (ii) in the low heme medium with no hemin added. We note that the low heme medium is not completely heme-free, as 10% FBS added to the medium supplements trace amount of heme. When cultured in the high heme medium, the PC cells RNAi-depleted for *Tb*Hrg did not show any significant growth defect as compared with the non-induced control (Fig. 3*A*). In contrast, the proliferation of the same cell line was significantly reduced in the low heme medium after RNAi induction (Fig. 3*B*). Further analysis of DNA by DAPI staining revealed a slight shift toward the non-dividing cells (1N1K) in the *Tb*Hrg knockdowns as compared with the wild-type strain induced in low heme medium for 10 days (data not shown).

To achieve complete elimination of the *Tb*Hrg protein, homologous recombination was used to generate knock-out cell line for both alleles of the single-copy *Tb*HRG gene (*Tb*Hrg KO). The *Tb*HRG alleles were replaced by either hygromycin or puromycin resistance cassettes, and the elimination of the target gene in the *Tb*Hrg KO cell line was confirmed by PCR using primers specific for *Tb*Hrg and α-tubulin as a control (Fig. 4*C*). This result showed that *Tb*Hrg is not essential for the viability of cultured PC *T. brucei*.

Down-regulation of TbHrg decreased heme content and heme uptake

To monitor changes in cellular heme levels upon the down-regulation of *Tb*Hrg, we employed an HPLC-based analysis. This methodology enabled accurate quantification of the non-covalently bound heme *b* and heme *a*, the latter being in *T. brucei* synthetized from heme *b* (33). In RNAi-induced *Tb*Hrg PC cells grown in the high heme medium, the heme *b* content was decreased by 30% when compared with the non-induced cells (Fig. 4*A*). This effect was even more pronounced during cultivation in the low heme medium, where heme *b* went down by 60% (Fig. 4*B*). The cellular concentration of heme *a* was more stable, showing no significant decrease in the PC *Tb*Hrg RNAi knockdowns grown in the high heme medium

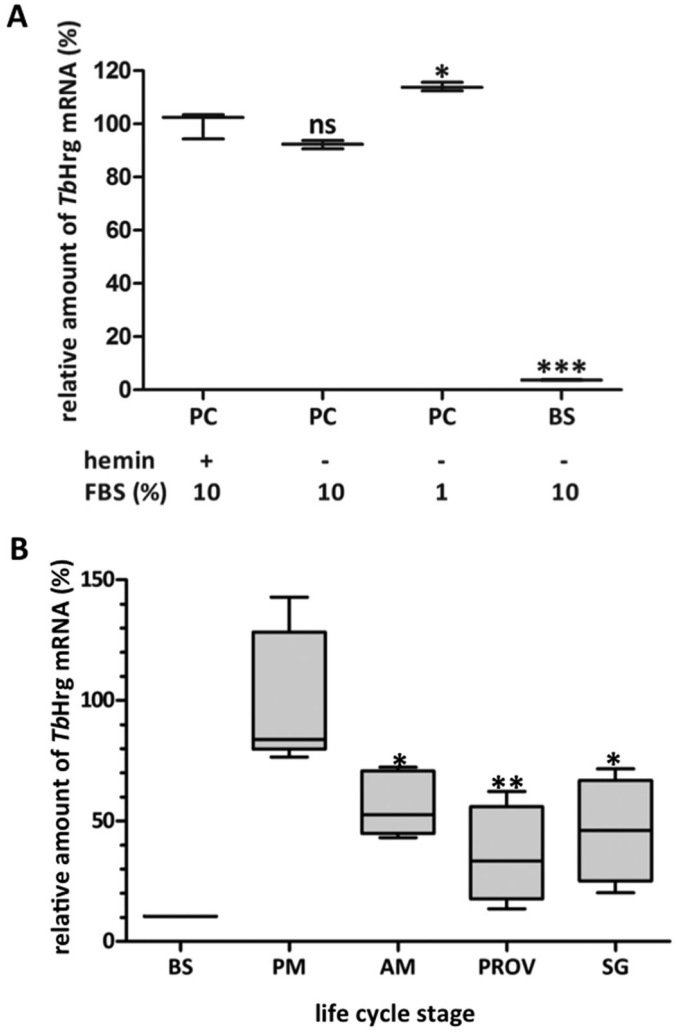

Figure 2. Comparative expression of *Tb*Hrg transcript in different developmental stages. *A*, quantitative real-time PCR of the *Tb*Hrg transcript in PC and BS of *T. brucei* 427 from axenic culture. Transcripts from wild type BS grown in 10% FBS and wild-type PC cells grown in 10% or 1% FBS were compared with PC cells grown in medium with 10% FBS and 11.4 μM hemin, which was set to 100%. Telomerase reverse transcriptase was used as an internal control. Statistical significance was determined by Student's *t* test with Welch's correction ($n = 3$; ns, $p > 0.05$; *, $p \leq 0.05$; ***, $p \leq 0.001$). *B*, quantitative real-time PCR of the *Tb*Hrg transcript in *T. brucei* AnTAR1 BS cells and in individually collected AnTAR1-infected tissues of *G. morsitans morsitans* flies: PM ($n = 5$), AM ($n = 5$), proventriculus/foregut (*PROV*) ($n = 4$), and SG ($n = 4$). The TERT (telomerase reverse transcriptase) and MRE11 housekeeping genes were used for normalization. Statistical significance was determined by Student's *t* test with Welch's correction (ns, $p > 0.05$; *, $p \leq 0.05$; **, $p \leq 0.01$; ***, $p \leq 0.001$). An overall test (all the groups) was done by a one-way analysis of variance (**, $p = 0.0023$).

(Fig. 4*A*). However, in the same cells grown in the low heme medium, heme *a* level was substantially decreased (by ~60%) (Fig. 4*B*).

Next, we have monitored the dynamics of heme uptake using ^{14}C-heme in *Tb*Hrg KO cells. In these trypanosomes, the uptake of radioactive heme was practically abolished, whereas in the wild types the radioactive heme content grew steadily to 1 ng/10^7 cells (Fig. 4*C*). This result strongly indicates that *Tb*Hrg has a key role in heme transport in PC *T. brucei* and that the transporter internalizes free heme, most likely as a solo player.

Depletion of TbHrg caused a change to mesocyclic-like morphology

The *Tb*Hrg KO cells underwent morphological changes, which were apparent already by standard light microscopy. Flagellates depleted for heme due to the absence of the *Tb*Hrg gene became markedly longer than the parental wild-type strain (Fig. 5, *A* and *B*). Statistical analysis of cell measurements documented that the *Tb*Hrg KO flagellates were almost twice as long as the wild-type PC cells. This also applies to the flagellum, which was prolonged, reflecting the particular extension of its attached part (Fig. 5*A*). Moreover, these morphological changes affected the shape of the single mitochondrion, which lost its reticulated structure and turned into a sausage-shaped organelle that resembled the mitochondrion of the BS cells (Fig. 5*C*). In the genetically modified trypanosomes, we also examined the relative position of the nucleus and the kinetoplast. Although the kinetoplast was often more distant from the elongated nucleus, it remained positioned in the posterior part of the cell, which is a defining feature of the PC morphology (Fig. 5*C*). All observed morphological changes hint to mesocyclic trypanosomes, which are found in the anterior midgut and proventriculus (34).

We observed a similar phenotype in the *Tb*Hrg RNAi strain when grown in low heme conditions for 10 days, although the emerging population was more heterogeneous in size and shape (Fig. 3*D*), with significant repositioning of the kinetoplast in respect to the nucleus. In ~40% of the *Tb*Hrg RNAi cells, the nucleus overlapped with the kinetoplast, and a minority of the cells (7%) had their kinetoplast positioned anterior to the nucleus. Such morphotypes were detected in the wild-type strain very rarely, with the majority of cells (98%) having the kinetoplast at the posterior end of the cell (Fig. 3*C*). The presence of an anterior kinetoplast would suggest the appearance of epimastigote stage, but we failed to detect the marker protein BARP in any of the cell lines studied (data not shown).

TbHrg KO cells are not compromised in tsetse flies

The *Tb*Hrg KO cells and the corresponding wild-type cells were further scrutinized *in vivo* within the tsetse fly vector. The establishment of PC infection of *Tb*Hrg KO in the tsetse fly midgut and the subsequent development of the trypanosomes into the infective metacyclic stage in the salivary glands were observed to be at similar level to the wild-type cells (Fig. 5*D*). The posterior midgut, where blood meal digestion takes place, is considered to be a heme-rich environment (35, 36), leaving the *Tb*Hrg KO cells unaffected. However, later the protists encounter a heme-low environment in the anterior midgut that stimulates the transformation into the mesocyclics stage, a predisposition already established in the *Tb*Hrg KO cells. Taken together, these results suggest that heme, either directly or indirectly through the downstream heme-based metabolic activity, may act as a regulator of *T. brucei* cell shape and differentiation.

TbHrg localizes to the flagellar pocket and membrane

To establish the intracellular localization of the *Tb*Hrg protein, BS and PC trypanosomes overexpressing the C-terminally tagged protein were generated using a tetracycline-inducible expression system. The production of *Tb*Hrg-V5 fusion protein

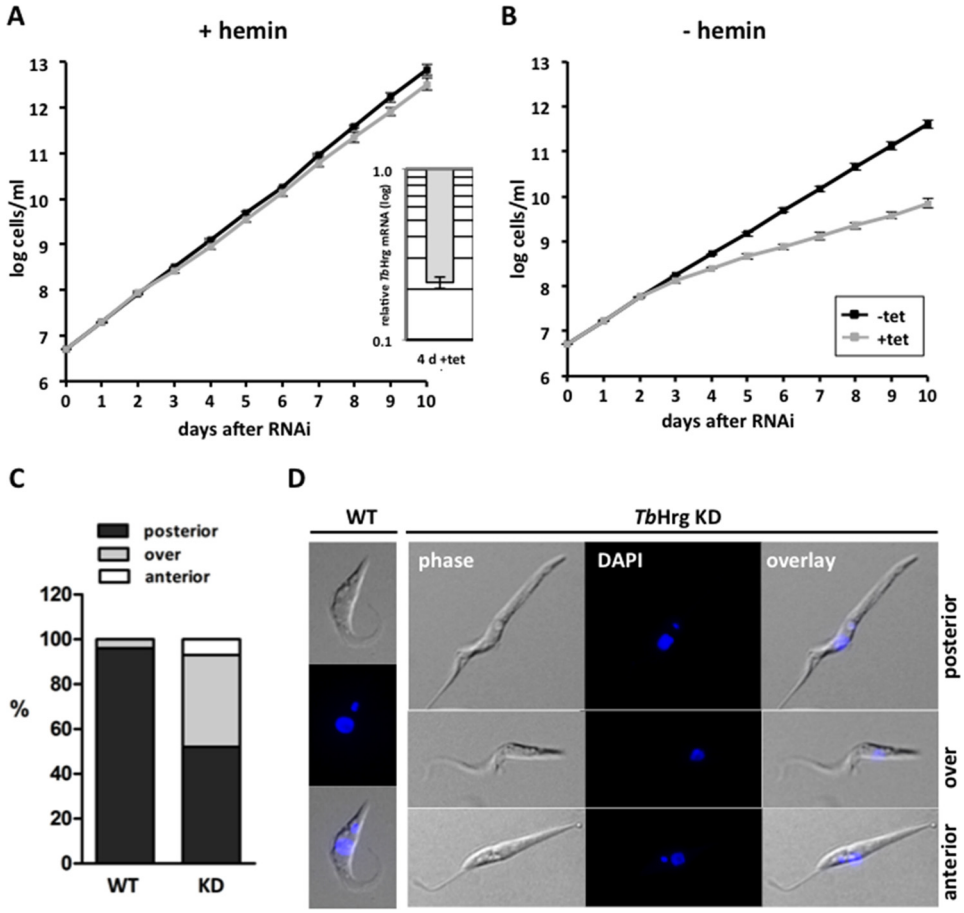

Figure 3. Down-regulation of *Tb*Hrg affects proliferation and kinetoplast positioning in low heme medium. Growth curves of non-induced (−*tet*; *black line*) and RNAi-induced (+*tet*; *gray line*) cells grown with 11.4 μM hemin (+*hemin*) (*A*) or in a medium without hemin (−*hemin*) (*B*). The *inset* shows verification of the *Tb*Hrg RNAi knockdown by quantitative real-time PCR. Total RNA was harvested from non-induced (−*tet*) and RNAi-induced (+*tet*, day 4) cells. *Tb*Hrg was compared with18S rRNA transcript, which was used as an internal control. *C*, mutual positions of nucleus and kinetoplast in wild type (*WT*) and *Tb*Hrg knock-down cells 10 days after RNAi induction (*KD*), respectively. The percentage calculated out of 200 cells per each strain is shown. *D*, fluorescence microscopy showing nuclear staining (*blue*) of representative cells from *panel C* with the kinetoplast positioned *posterior* or *anterior* with respect to the nucleus or overlapping with it (*over*).

was verified by Western blot analysis in both life cycle stages (Fig. 6*A*) with the expression higher in the PC flagellates as compared with the BS flagellates. Notably, in the SDS-PAGE gel the protein migrated at ~120 kDa, although its predicted size along with the V5 tag is ~20 kDa (Fig. 6*A*). This mobility shift was most likely caused by extreme hydrophobicity of this membrane protein, which contains four transmembrane domains. Additionally, we used LDS-PAGE to better resolve the protein, and indeed the V5-signal correlated with molecular mass of 20 kDa (data not shown).

The cell lines overexpressing *Tb*Hrg-V5 were further studied by light and electron microscopy. Upon decoration with monoclonal α-V5 antibody, immunofluorescence microscopy localized the signal within the flagellum in both the PC and BS cells (Fig. 6*B*). The same approach, but with the methanol-permeabilization step omitted, located all the V5-tagged *Tb*Hrg protein to the same cellular compartment (data not shown). Hence, the *Tb*Hrg protein seems to be incorporated into the surface layer of the flagellum as part of its membrane. Moreover, the flagellar pocket also contained a fraction of the fluorescent signal (Fig. 6*B*). In the BS cells, signals could additionally be detected in the intracellular vesicles compatible with the endocytic compartments, suggesting a possible role of the transporter in heme mobilization across the endomembrane systems downstream of the HpHb cargo delivery in the acidic compartments (Fig. 6*B*), in agreement with previous findings (25).

Next, the PC cell line overexpressing V5-tagged *Tb*Hrg was subjected to immunostaining with primary α-V5 and secondary α-mouse gold-labeled antibodies followed by scanning electron microscopy. This sensitive technique confirmed the presence of *Tb*Hrg in the flagellar membrane with the pixels progressively increasing toward the flagellar pocket (Fig. 6*C*, *1–3*), as compared with the wild-type strain where no pixels were detected (Fig. 6*C*, *4*). This approach did not enable detection of the tagged protein within the flagellar pocket but provided evidence for its presence on the surface of the flagellum (Fig. 6*C*).

To rule out possible artifacts caused by protein overexpression, a PC cell line was generated that carried endogenously tagged *Tb*Hrg with the V5 tag attached to its C terminus (Fig. 6*A*). We examined the intracellular localization of the endogenously tagged protein, which is essentially the same as in the *Tb*Hrg-overexpressing cell line, as most of the signal

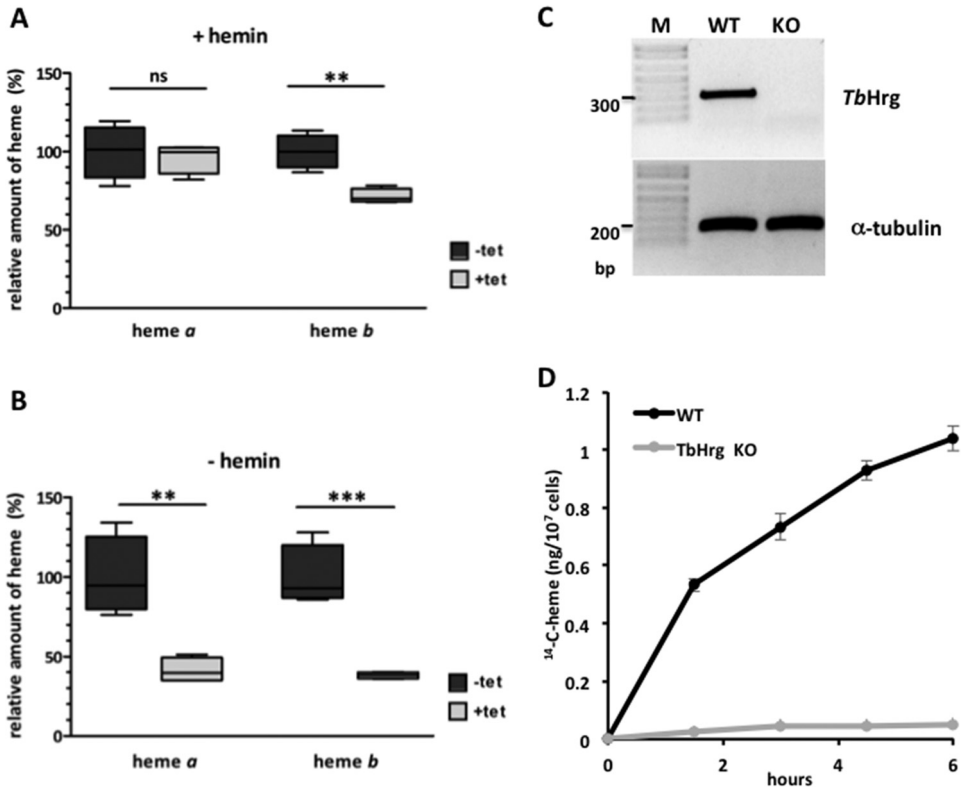

Figure 4. Heme content and uptake is affected in *Tb*Hrg KD and KO cells. Relative heme content (*heme a* and *heme b*) in the non-induced (−*tet*, *dark gray columns*) and RNAi-induced (+*tet*, day 4, *light gray columns*) cells grown in the presence of 11.4 μM hemin (*A*) or its absence (*B*). Heme content in the non-induced cells was set to 100%. Heme was extracted from 1×10^9 flagellates, separated by HPLC, and detected by diode array detector. Statistical significance was determined by Student's *t* test with Welch's correction ($n = 4$; ns, $p > 0.05$, **, $p \leq 0.01$; ***, $p \leq 0.001$). *C*, verification of *Tb*Hrg knock-out (*KO*) cells. Genomic DNA was isolated from the wild type (*WT*) and *Tb*Hrg KO cells and PCR-amplified with specific primers for part of the *Tb*Hrg and α tubulin genes, with the latter used as a control. The amplicons were visualized in an ethidium bromide-stained agarose gel. *D*, dynamic accumulation of ^{14}C-heme in WT (*black line*) and *Tb*Hrg KO cells (*gray line*) is shown. WT and *Tb*Hrg KO cells were incubated with ^{14}C-heme, which was quantified in each sample by Beckman Coulter LS 6500 scintillation counter.

decorates the flagellar membrane and the flagellar pocket (Fig. 6*B*).

Overexpression of TbHrg led to accumulation of heme in BS

In *L. amazonensis*, overexpression of Lhr1 led to elevated uptake of heme analog zinc protoporphyrin (22). We tried to use the same approach for *T. brucei*, but the zinc protoporphyrin did not enter live cells. Therefore, we decided to employ another methodology using radioactively C^{14}-labeled heme, and this way the dynamics of heme accumulation in the verified BS *Tb*Hrg-V5 cells could be followed. Indeed, flagellates overexpressing the V5-tagged protein showed a substantially higher ability to internalize heme as compared with their wild type counterparts (Fig. 7*A*). After 24 h of RNAi induction, 2× more radioactive heme accumulated in the former cells as compared with the wild-type cells (Fig. 7*A*).

Overexpression of TbHrg triggers a switch of procyclins in PC

PC cells expressing *Tb*Hrg-V5 were monitored for their surface procyclins. By Western blot analysis, the overexpression of *Tb*Hrg-V5 reproducibly triggered strong up-regulation of early procyclin GPEET with the concomitant decrease of the late procyclin EP1 (Fig. 7*B*). The switch was apparent already in the non-induced cells probably due to a leaky tetracycline-inducible expression system. In the wild-type cells, the GPEET protein was almost undetectable, yet after 24 h of tetracycline induction, a 5-fold increase of GPEET occurred. On the contrary, EP1 was negligible in the cells induced for 24 h, 10× lower compared with wild-type levels (Fig. 7*B*). Combined, the results indicated that *Tb*Hrg might play a role in the life cycle progression, in particular in driving the complex morphological changes associated with the move of the infection from the midgut into the proventriculus.

Discussion

Progress in understanding heme homeostasis in most eukaryotic systems is often hampered by the inability to separate heme biosynthesis from downstream intracellular transport pathways. We bypassed this problem by using genetically tractable *T. brucei*, which is unable to synthesize heme but instead relies on heme scavenged from its hosts (1, 5, 37), whereas few related trypanosomatids likely acquire heme from their bacterial endosymbionts (38). Interestingly, another trypanosomatid-parasitizing plant, *Phytomonas serpens*, was recently shown to survive without any heme, the first example of its kind among aerobic eukaryotes (39). This is certainly not the case of PC *T. brucei*, which contains over a dozen essential heme-carrying proteins (9, 37, 39, 40).

Despite its overall essentiality and versatility, heme has high cellular toxicity due to its iron-induced effect on DNA, proteins, and membrane lipids (41). Therefore, to reduce the deleterious effects of free heme, every prokaryotic and eukaryotic

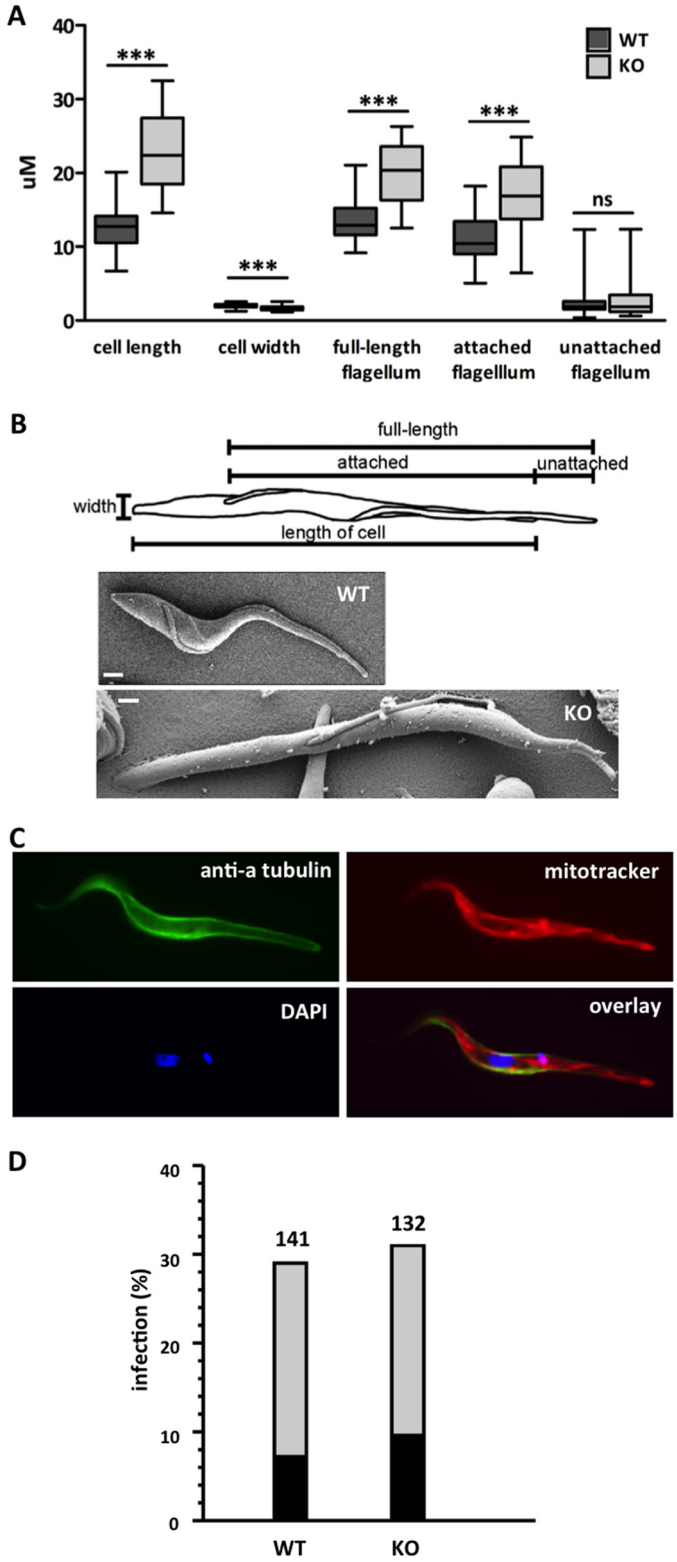

Figure 5. TbHrg KO cells with mesocyclic-like morphology are not compromised in tsetse flies. *A*, comparison of morphology of wild type (*WT*) (*dark gray column*, $N_{cells} = 40$) and *Tb*Hrg KO cells (*KO*) (*light gray column*, $N_{cells} = 37$) grown in low heme medium for 10 days. Statistical significance was determined by Student's *t* test (ns, $p > 0.05$; ***, $p \leq 0.001$). *B*, schematic representation of measurements from the graph shown in Fig. 3*A*. Scanning electron microscopy of WT (*upper panel*) and KO cells (*lower panel*). The *bar* is 1 μm. *C*, immunofluorescence assay of PC *Tb*Hrg KO cells grown in the low heme medium for 10 days, stained with DAPI (*blue*), α-tubulin antibody (*green*), and MitoTracker (*red*). *D*, infection rates at day 28 post-infection of *G. morsitans morsitans* flies with the WT (AnTAR1) and *Tb*Hrg KO PC cells. *Gray column*: established midgut infection; *black column*: % maturation of midgut-infected flies; *n* = number of dissected flies.

cell tightly regulates its uptake and storage. Transport and distribution of heme in trypanosomatids remain elusive, although several high affinity heme-binding proteins were identified that allow active heme uptake (1, 9, 37, 40). The HpHb complex, internalized by the HpHbR, is the main source of heme for BS *T. brucei* (9). HpHbR is conspicuously missing from the PC cells. Consequently, the PC cells were predicted to acquire free heme by other means than via the HpHb complex (9).

Here we show *in vitro* and *in vivo* that *Tb*Hrg functions as the free-heme transporter with an expression pattern complementary to HpHbR, with *Tb*Hrg being abundant in PC yet negligible in BS *T. brucei*. Somewhat unexpectedly, the abundance of the *Tb*Hrg transcript was not modulated by heme availability. This is, however, not unprecedented, as there are other heme transporters in *C. elegans*, which are constitutively expressed and not at all regulated by heme (42). Unlike in the BS cells, where the down-regulation of *Tb*Hrg appears lethal (25), we found that its RNAi-mediated targeting in PC causes growth phenotype only under low heme conditions. The BS cells have been proposed to use *Tb*Hrg for transportation of endocytosed heme from the lysosome into the cytoplasm (25). The fact that endocytosis is up-regulated in BS as compared with PC (43) may explain the differences in viability between these two stages.

It was reported that in *Leishmania donovani* high concentration of heme reduced the level of protein synthesis, namely of β-tubulin with a concomitant up-regulation of heat shock protein 90 (36). Moreover, morphological changes similar to *in situ* transformation from the promastigote stage to the macrophage-dwelling amastigote stage were observed which suggested that heme may be the key factor triggering transformation of these flagellates (44). Similar modulation by heme concentration was later reported in *T. cruzi*, which responded to high heme concentration with decreased growth rate, followed by the transformation of the epimastigotes into amastigotes (45). Moreover, heme was recently found to be a regulatory molecule affecting the eIF2α kinase2 activity and regulating development in the insect form of *T. cruzi* (46).

Our observations support an important role of heme in the life cycle progression of *T. brucei*, as the disruption of *Tb*Hrg decreased intracellular heme and eventually led to its disappearance. The extremely low heme environment may mimic the challenging conditions in the anterior midgut and proventriculus of the tsetse fly, where transformation of the PC trypanosomes into the mesocyclic stage occurs. We noticed a substantially prolonged cell shape of the *Tb*Hrg KO cells, although the kinetoplast and the nucleus remained in positions characteristic for the PC cells, contrary to the *Tb*Hrg RNAi knockdown cells in which the kinetoplast moved toward the anterior end of the cell. The length of the free flagellum was not altered by the absence of *Tb*Hrg, whereas the flagellum attachment zone grew significantly. This is an important feature, as the length of the attachment zone was recently shown to be a key regulator of trypanosome cell shape (47, 48). Additionally, we provide evidence that *Tb*Hrg KO mutant could colonize the

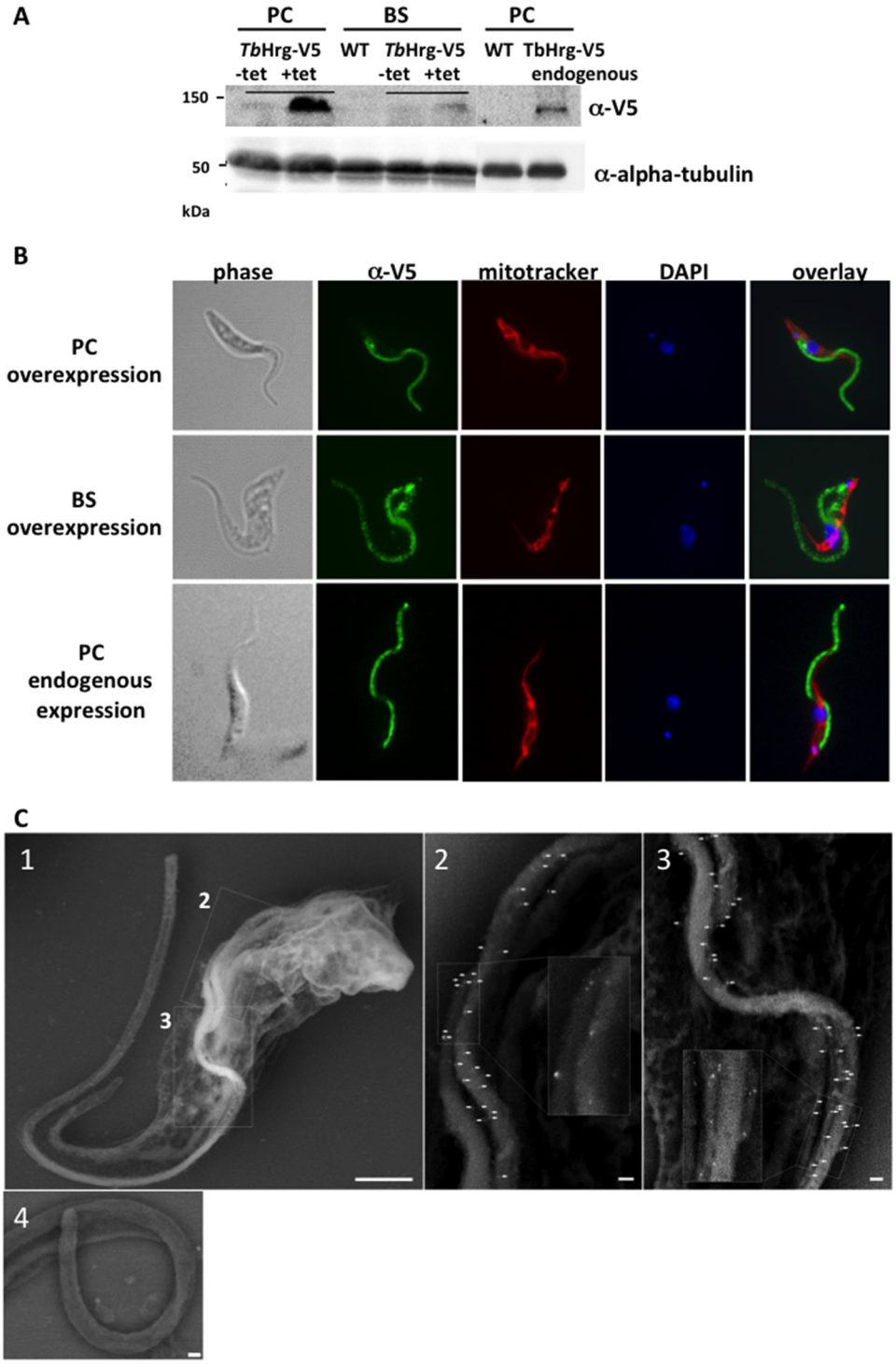

Figure 6. TbHrg localizes into the flagellar membrane and pocket. *A*, overexpression and endogenous expression of the C-terminally V5-tagged *Tb*Hrg in PC and BS flagellates. Western blot analysis with α-V5 antibody shows the absence and presence of the tagged protein in non-induced (−*tet*) and induced cells (+*tet*, day 1), respectively. α-Tubulin was used as a loading control. *B*, immunofluorescence assay of C-terminally V5-tagged *Tb*Hrg in PC and BS cells, which were stained with monoclonal α-V5 antibody (*green*), MitoTracker (*red*), and DAPI (*blue*). *C*, scanning electron microscopy of PC cells overexpressing the C-terminally V5-tagged *Tb*Hrg. Processing for scanning microscopy was followed by immunodecoration with α-V5 antibody labeled with gold nanoparticles (1.4 nm in diameter). *1*, low magnification view imaged using secondary electrons. *2* and *3*, silver-enhanced nanoparticles were observed using back-scattered electrons. Varying density of nanoparticles on the flagellar membrane in different parts of flagellum is shown by *white arrows*. *Bars* are 1 μm (*1*) and 100 nm (*2* and *3*). *4*, wild type cells immunodecorated with α-V5 antibody attached to gold nanoparticles, used as a negative control, lacked any signal. The *bar* is 100 nm.

tsetse flies at rates and intensities comparable with the wild-type cells.

Furthermore, we show here that the overexpression of *Tb*Hrg-V5 causes a dramatic increase of GPEET accompanied by a concurrent drop of the EP1 procyclin. The developmental regulation of surface proteins expression in PC has been extensively studied (49, 50). Upon ingestion by the tsetse fly, developmentally competent stumpy forms readily transform into the

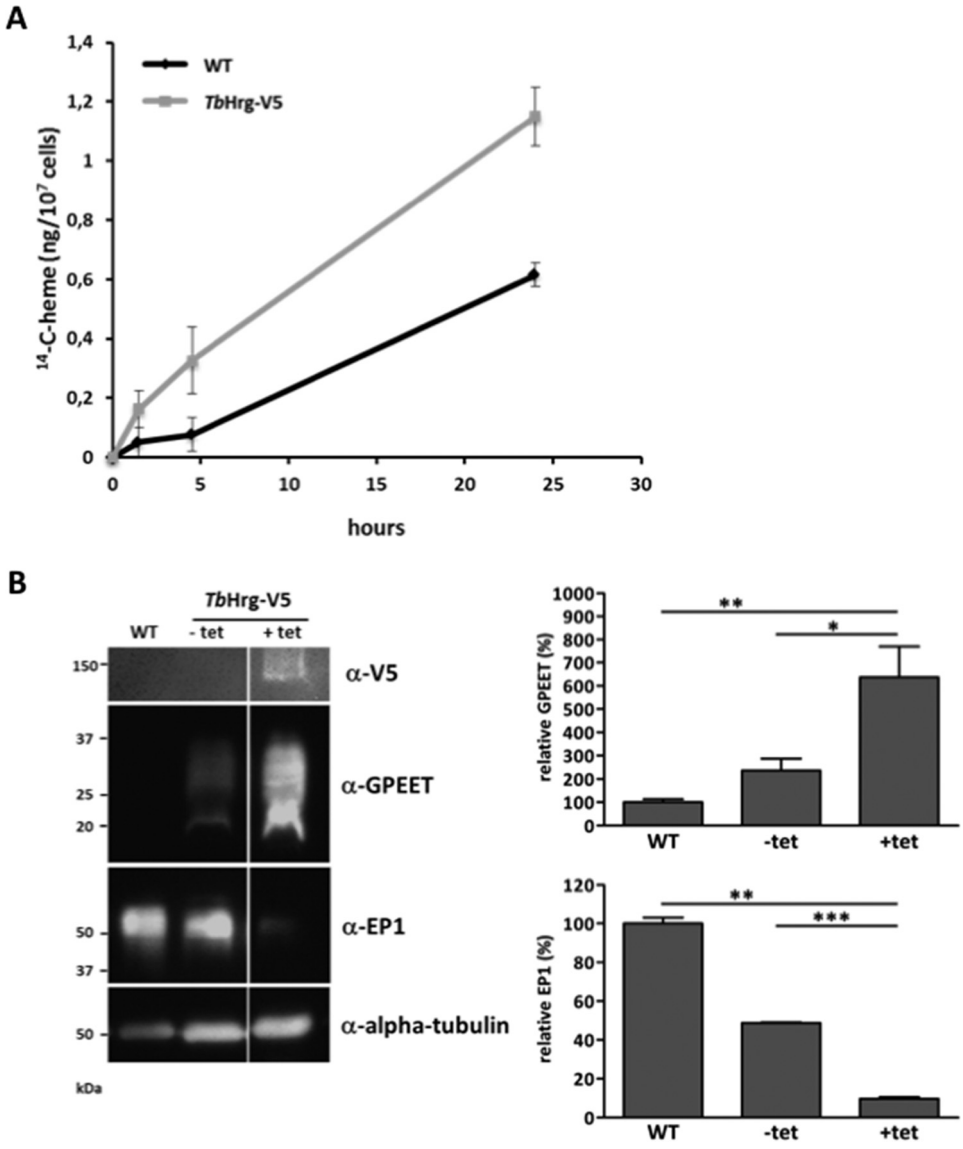

Figure 7. Overexpression of *Tb*Hrg-V5 leads to accumulation of heme in BS cells and switch of procyclins in PC cells. *A*, dynamic accumulations of radioactive ^{14}C-heme in WT BS cells (*black line*) and in those overexpressing *Tb*Hrg-V5 (*gray line*). Cells incubated with ^{14}C-heme were quantified by scintillation. *B*, Western blot analysis of wild type (*WT*) PC cells and those overexpressing V5-tagged *Tb*Hrg, non-induced (−*tet*), and RNAi-induced cells (+*tet*, 24 h). Their lysates were immunodecorated with antibodies against the early GPEET procyclin and the late EP1 procyclin as well as with α-tubulin antibodies, used as a loading control. The overexpression of *Tb*Hrg-V5 was monitored with α-V5 antibodies. Statistical significance for GPEET ($n = 3$) and EP1 ($n = 2$) protein expression (WT value set to 100%) was determined by Student's *t* test (*, $p \leq 0.05$; **, $p \leq 0.01$, ***, $p \leq 0.001$).

early PC cells expressing both the GPEET and EP procyclins. During the first days of midgut colonization, GPEET will largely dominate the surface coat. At a later stage, under the control of undetermined environmental stimuli, the surface coat will be replaced by the EP procyclins. *In vitro* studies have revealed that the switch from GPEET to EP could be accelerated under hypoxic conditions or prevented by the addition of exogenous glycerol (51). We demonstrate here that the *Tb*Hrg function and heme bioavailability act as positive regulators of the early GPEET procyclins. Compatible with these observations, the GPEET-to-EP transition in the tsetse fly occurs after the completion of the blood meal digestion, leaving behind the PC flagellates in a heme-depleted midgut. We hypothesize that this heme-rich to heme-poor transition could, via *Tb*Hrg, trigger cellular differentiation.

In *L. amazonensis* and BS *T. brucei*, Hrg localizes to the plasma membrane and to endocytic compartments, respectively (22, 25). Moreover, it was also found in the flagellar pocket region in *T. cruzi*, indicating possible regulation of heme uptake in this compartment (23). In PC and BS *T. brucei*, we observed the *Tb*Hrg protein in the endocytic vesicles associated with the flagellar pocket but additionally found it also in the flagellar membrane. This unanticipated localization was functionally confirmed by the increased uptake of heme upon the overexpression of the tagged *Tb*Hrg. A further line of evidence verifying the flagellar localization was obtained from a PC strain with endogenously V5-tagged *Tb*Hrg. Very little is known about sensing and signaling in the flagellum, but proteins regulated by Ca^{2+} have previously been localized in the *T. brucei* flagellum (52), lending additional support to its putative sensing capacity.

Collectively, we present first evidence that in PC *T. brucei* heme is acquired via flagellum-located *Tb*Hrg, implying that heme has to be transported into the cytoplasm through the flagellar membrane and flagellar pocket. Moreover, it is plausible that heme is one of the environmental stimuli that is involved in the transformation of this important human parasite during its journey through the midgut of the tsetse fly vector.

Experimental procedures

Quantitative real-time PCR

Total RNA from each cell line was isolated using TRI reagent (MRC). To remove residual DNA, the DNase treatment was performed using the Turbo DNA-free DNase kit (Ambion). The SuperScriptIII reverse transcriptase (Invitrogen) and oligo$(dT)_{20}$ (Invitrogen) were used to generate cDNA. Quantitative real-time PCR was performed as described elsewhere (53). The primer pair TbHrg-QP-FW (5′-GTGGACGGGTGAATCCAACT) and TbHrg-QP-RV (5′-ACAACATGCTCGTCTGAGGG) was used to detect the *Tb*Hrg mRNA. The primer pair of telomerase reverse transcriptase was used as internal reference following a protocol described elsewhere (54). The relative *Tb*Hrg mRNA abundance between either the RNAi-induced and non-induced cells or the PC and BS cells was determined by the Pfaffl method (55).

Preparation of cell line overexpressing V5-tagged TbHrg

The full-length *Tb*Hrg (Tb927.8.6010) gene without stop codon was PCR-amplified from the *T. brucei* genomic DNA using primer pair TbHrg_HindIII_FW (5′-CGCAAGCTTATGGCTCTTTCAGAGAAAGC) and TbHrg_BamHI_RV (5′-CGCGGATCCCAACATGCTCGTCTGAGGGC) (the added restriction sites BamHI and HindIII are underlined). The amplicon was subsequently cloned into pT7V5 plasmid and verified by sequencing. The *Tb*Hrg-V5 contains V5 tag at its C terminus. The construct was linearized by NotI and then transfected into *T. brucei* 29–13 (PC) using BTX electroporator and selected as described elsewhere (56). The construct was also electroporated into *T. brucei* 427 (BS) cell using the Amaxa Nucleofector II electroporator, with transfectants maintained in HMI-9 medium and selected following a protocol described previously (53). The expression of the *Tb*Hrg-V5 protein tagged was initiated by the addition of 1 μg/ml tetracycline to the medium.

Preparation of cell line with endogenous V5-tagged TbHrg

Primers were designed according to the protocol for endogenous C-terminal tagging (57). Used primers for *Tb*Hrg are the following: TbHrg_FW_GFPc_pPOT (5′-ACCCCATCTAACCCACCCGAATTCGACAGTTTACGTAAGGGGGAAGAAGAGGTAACGGAAAGGAGGGCCCTCAGACGAGCATGTTGGGTTCTGGTAGTGGTTCC) and TbHrg_RV_GFPc_pPOT (5′-TCACGCGAGTCTTTTCTTCATTCTCTCATAGAAGTGGGGAGTTTCATCACGGACAGGGTGCCGCTGTTGATGCGCTCCAGGTGTCCCAATTTGAGAGACCTGTGC). We modified pPOTv4 by replacing the enhanced YFP with 3× V5 tag. The product for electroporation was amplified by PCR according to the published protocol and directly used for the electroporation of SmOxP9 cells (57).

Western blot analysis

Cell were harvested at the density 2–5 × 10^6 cells/ml and lysed. Lysates (5 × 10^6 cells) were loaded on a 15% SDS-PAGE gel and proteins were subsequently transferred to the PVDF membrane. The membrane was incubated with primary antibodies, the monoclonal α-V5 antibody (Invitrogen), polyclonal K1 α-GPEET antibody (provided by Isabel Roditi) and polyclonal antibody against enolase (provided by Paul A. M. Michels), using 1:1,000, 1:1,000 and 1:200,000 dilutions, respectively. The membrane was subsequently incubated with appropriate secondary antibodies conjugated with horseradish peroxidase (Sigma) and visualized using Clarity western ECL substrate (Bio-Rad).

Growth curves

PC cells were routinely grown in SDM-79 media which contains 11.4 μM hemin and 10% fetal calf serum (FBS). Cells were placed in media with different heme content and the measurements started after 24 h incubation in different heme conditions. Cell densities were measured daily using cell counter and diluted back to density 5 × 10^6/ml.

Production of ^{14}C-heme and heme uptake assay

The *E. coli* AN344/pTYR13 was grown in LB medium with 12 μM ferric citrate, 35 mg of ampicillin/liter and 31 μM of 50–60 mCi/mmol 5-[4-^{14}C]aminolevulinic acid (American Radiolabeled Chemicals). Isolation of ^{14}C-heme was done according to a protocol described elsewhere (58). Heme concentration was measured using pyridine hemochrome assay. The purified ^{14}C-heme (~370 Ci/mol) was used in heme uptake assay (see below). The PC (10^7 cells/ml) and BS flagellates (8 × 10^5 cells/ml) were incubated in SDM-79 and HMI-9 media, respectively, which contained 1% FBS and were supplemented with 0.031 μg/ml of ^{14}C-heme. Cells were harvested by centrifugation through oil (dibutyl phthalate: phthalic acid bis(2-ethylhexyl ester) in a ratio 2:1 v/v) and at each time point, the pellet was subsequently added to Ecoscint H (National Diagnostics) scintillation solution. The radioactivity was determined by liquid scintillation using Beckman LS 6500.

Generation of TbHrg RNAi cell lines and cultivation

A 301-nt long fragment of *Tb*Hrg was PCR-amplified from the *T. brucei* genomic DNA, strain 29–13, using primer pair TbHrg_BamHI_FW (5′-GCGGGATCCAGAGAAAGCGTGTCTCCGAA) and TbHrg_XhoI_RV (5′-GCGCTCGAGGCGCCTCTTAATACCAACCA) (added BamHI and XhoI restriction sites are underlined). The amplicon was subsequently cloned into the vector p2T7–177, which was subsequently electroporated into the *T. brucei* strain 29–13. Electroporation and selection were performed following a protocol described previously (50). The PC cells were cultivated in SDM-79 medium at 27 °C. The RNAi of *Tb*Hrg transcript was induced by the addition of 1 μg/ml of tetracycline to the medium. Cell growth was measured by the Beckman Z2 Coulter counter at 24 h intervals.

Generation of TbHrg knock-out cell lines

A 500-nt-long fragment of 5′- and 3′-UTR of *Tb*Hrg was PCR-amplified using primer pairs 5′-UTR_XhoI_FW (5′-CGCCTCGAGAGAGGCGTTTGTGGCTTCTC) and 5′-UTR_XbaI_RV (5′-CGCTCTAGATTTCTCTTATTTATTCACTCTTGACTTAT) (added XhoI and XbaI restriction sites are underlined) and 3′-UTR_BamHI_FW (5′-CGCGGATCCGACACCTGGAGCGCATCAAC) and 3′-flanking_XhoI_RV (5′-CGCCTCGAGACGGAACTCGTGAGATGCCA) (added BamHI and XhoI restriction sites are underlined). The amplicons were subsequently cloned into the plasmids pUCKO-HYG and pUCKO-PURO carrying the hygromycin and puromycin resistance genes, respectively, resulting in pUCKO-HYG-TbHrgKO and pUCKO-PURO-TbHrgKO constructs. After linearization with XhoI, the pUCKO-HYG-TbHrgKO cassette was transfected into the PC *T. brucei* to replace the first *Tb*Hrg allele. The single-allele knock-out (KO) cells were subsequently transfected with the pUCKO-PURO-TbHrgKO cassette to obtain the *Tb*Hrg KO cells. Primer pairs TbHrg_FW_HindIII and TbHrg_RV_BamHI and tubulin_FW (5′-GAAGGAGGTTGATGAGCAGATGC) and tubulin_RV (5′-TACCAGTGCAAGAACGCCTTG) (used as control) were used to verify deletion of both *Tb*Hrg alleles.

Heme measurement

The experiment was started after cultivation of cells in SDM-79 medium with or without additional hemin for 1 day. A total 1×10^9 PC cells (non-induced, RNAi induced for 4 days) were harvested and washed 3 times with phosphate-buffered saline. The pellet was then resuspended in 60 μl of H_2O and extracted with 400 μl of acetone, 0.2% HCl. The supernatant was collected after centrifugation for 5 min at 12,000 rpm. The pellet was resuspended in 200 μl of acetone, 0.2% HCl and centrifuged again for 5 min at 12,000 rpm. Both supernatants were combined, and 150 μl of each sample was immediately injected onto an HPLC machine (Agilent-1200) and separated using a reverse phase column (4 μm particle size, 3.9 × 75 mm, Waters) with 0.1% trifluoroacetic acid and acetonitrile, 0.1% trifluoroacetic acid as solvents A and B, respectively. Both heme *a* and *b* were eluted with a linear gradient of solvent B (30–100% in 12 min) followed by 100% of B at a flow rate of 0.8 ml/min at 40 °C. Heme *a* and *b* were detected by diode array detector Agilent 1200 (Agilent Technologies) and identified by retention time and absorbance spectra according to commercially available standards (Sigma).

Immunofluorescence assay

Approximately 1×10^7 PC and BS cells were harvested and centrifuged, and the cell pellet was resuspended in a fresh medium. Before the fixation step, cells were labeled with mitochondrial marker MitoTracker Red (20 nM). The following steps were done according to the protocol described previously (27). The samples were visualized using an Axioplan2 imaging (Zeiss) fluorescent microscope.

Scanning electron microscopy

For immunolabeling, cells were centrifuged (1140 × *g*, 10 min, 4 °C), washed in 0.1 M Hepes buffer, and fixed in 4% formaldehyde for 1 h at room temperature. Cells were 3 times washed in Hepes, 0.01 M glycine, centrifuged, and transferred to glass slides. Prior this step, the slides were washed in ethanol, coated by a thick carbon layer, thoroughly rinsed in ethanol, and dried at 60 °C for 48 h. Finally, slides were glow-discharged for 30 s to make their surface hydrophilic and were immediately used. Cells were left to adhere for 10 min and were then incubated in 5% low-fat milk, 0.01 M glycine in Hepes for 2 h at room temperature. Mouse monoclonal antibody against the V5 tag (Invitrogen) was diluted in the blocking solution (25 μg/ml). After washing, the cells were incubated for 1 h with Alexa fluor 488 FluoroNanogold Fab anti-mouse IgG (Nanoprobes) diluted in the block solution to final concentration 2.5 μg/ml. Next, cells were washed in Hepes and deionized water (3 × 5 min). For silver enhancement, the HQ Silver kit (Nanoprobes) was used according to the manufacturer's instructions; the incubation time was 2 min. Cells were rinsed in deionized water (3 × 5 min), post-fixed in 2% osmium tetroxide for 30 min, washed in deionized water (3 × 5 min), and dehydrated in a graded series of acetone (30%, 50%, 70%, 80%, 90%, 100%; 4 min in each step). The samples were dried using critical point drying (CPD2 Pelco). Finally, slides were carbon-coated and observed in a scanning electron microscope JSM 7401-F (JEOL) equipped with Autrata YAG/BSE detector at an accelerating voltage 4–6 kV, working distance 9 mm, beam current 10–20 μA and imaged using both secondary and backscattered electrons. Cells for length measurements were fixed in 2.5% glutaraldehyde in 0.1 M phosphate buffer overnight at 4 °C. After three washing steps in 0.1 M phosphate buffer with 4% glucose, pelleted cells were transferred to poly-L-lysine-coated slides, post-fixed using 1% osmium tetroxide for 2 h at room temperature, washed, and dehydrated in the graded series of acetone for 15 min at each step. Finally, samples were critical point-dried (CPD2 Pelco™, Ted Pella), mounted on aluminum stubs, gold-coated (sputter coater Bal-tec SCD 050, Leica), and examined as described above. The length of both the flagellum (unattached and full-length) and the cells were measured using Image J software (rsbweb.nih.gov), and the obtained results were statistically evaluated.

Fly infection

Freshly emerged *Glossina morsitans morsitans* male tsetse flies were used in the infection experiments. Within 24–48 h after their emergence, flies were fed their first blood meal through *in vitro* membrane feeding on a mixture of saline-washed horse red blood cells (E&O Laboratories) with PC trypanosomes in SDM79 culture medium (without antibiotics) at a final concentration of 2×10^6 cells/ml. Only fully engorged flies were selected and subsequently maintained for 30 days by feeding 3 times per week on sterile defibrinated horse blood. Then, different parts of the alimentary tract (posterior midgut, anterior midgut, proventriculus/foregut) and the salivary glands were dissected and collected in 1 ml of TRIzol for RNA extraction.

Statistical analyses

Statistical significance was determined by one-way analysis of variance for multiple comparisons and by Student's *t* test with Welch's correction for one-to-one comparison using GraphPad Prism software.

Author contributions—E. H. and P. C. conducted most of the experiments, analyzed the results, and wrote most of the paper. M. V. conducted the transmission and scanning electron microscopy experiments. R. S. conducted the heme experiments measured by HPLC. J. V. D. A. conducted the fly experiments. B. V. supervised the work and edited the manuscript. J. L. conceived the idea for the project and edited the manuscript.

Acknowledgments—Antibodies were kindly provided by Isabel Roditi (University of Bern) and Paul A. M. Michels (University of Edinburgh). We thank L. Hederstedt (Lund University) for advice on heme radiolabeling.

References

1. Kořený, L., Oborník, M., and Lukeš, J. (2013) Make it, take it, or leave it: heme metabolism of parasites. *PLoS Pathog.* **9,** e1003088
2. Mense, S. M., and Zhang, L. (2006) Heme: a versatile signaling molecule controlling the activities of diverse regulators ranging from transcription factors to MAP kinases. *Cell Res.* **16,** 681–692
3. Panek, H., and O'Brian, M. R. (2002) A whole genome view of prokaryotic haem biosynthesis. *Microbiology* **148,** 2273–2282
4. Oborník, M., and Green, B. R. (2005) Mosaic origin of the heme biosynthesis pathway in photosynthetic eukaryotes. *Mol. Biol. Evol.* **22,** 2343–2353
5. Kořený, L., Lukeš, J., and Oborník, M. (2010) Evolution of the haem synthetic pathway in kinetoplastid flagellates: an essential pathway that is not essential after all? *Int. J. Parasitol.* **40,** 149–156
6. Tripodi, K. E., Menendez Bravo, S. M., and Cricco, J. A. (2011) Role of heme and heme-proteins in trypanosomatid essential metabolic pathways. *Enzyme Res.* **2011,** 873230
7. Ferguson, M. A., and Homans, S. W. (1988) Parasite glycoconjugates: towards the exploitation of their structure. *Parasite Immunol.* **10,** 465–479
8. Wassell, J. (2000) Haptoglobin: function and polymorphism. *Clin. Lab.* **46,** 547–552
9. Vanhollebeke, B., De Muylder, G., Nielsen, M. J., Pays, A., Tebabi, P., Dieu, M., Raes, M., Moestrup, S. K., and Pays, E. (2008) A haptoglobin-hemoglobin receptor conveys innate immunity to *Trypanosoma brucei* in humans. *Science* **320,** 677–681
10. Roditi, I., Schwarz, H., Pearson, T. W., Beecroft, R. P., Liu, M. K., Richardson, J. P., Bühring, H. J., Pleiss, J., Bülow, R., and Williams, R. O. (1989) Procyclin gene expression and loss of the variant surface glycoprotein during differentiation of *Trypanosoma brucei*. *J. Cell Biol.* **108,** 737–746
11. Vanhollebeke, B., Uzureau, P., Monteyne, D., Pérez-Morga, D., and Pays, E. (2010) Cellular and molecular remodeling of the endocytic pathway during differentiation of *Trypanosoma brucei* bloodstream forms. *Eukaryot. Cell* **9,** 1272–1282
12. van Hellemond, J. J., Opperdoes, F. R., and Tielens, A. G. (2005) The extraordinary mitochondrion and unusual citric acid cycle in *Trypanosoma brucei*. *Biochem. Soc. Trans.* **33,** 967–971
13. Verner, Z., Basu, S., Benz, C., Dixit, S., Dobáková, E., Faktorová, D., Hashimi, H., Horáková, E., Huang, Z., Paris, Z., Peña-Diaz, P., Ridlon, L., Týč, J., Wildridge, D., Zíková, A., and Lukeš, J. (2015) Malleable mitochondrion of *Trypanosoma brucei*. *Int. Rev. Cell Mol. Biol.* **315,** 73–151
14. Toh, S. Q., Glanfield, A., Gobert, G. N., and Jones, M. K. (2010) Heme and blood-feeding parasites: friends or foes? *Parasit. Vectors.* **3,** 108
15. Ooi, C. P., and Bastin, P. (2013) More than meets the eye: understanding *Trypanosoma brucei* morphology in the tsetse. *Front. Cell Infect. Microbiol.* **3,** 71
16. Van Den Abbeele, J., Claes, Y., van Bockstaele, D., Le Ray, D., and Coosemans, M. (1999) Trypanosoma brucei spp. development in the tsetse fly: characterization of the post-mesocyclic stages in the foregut and proboscis. *Parasitology* **118,** 469–478
17. Tracz, M. J., Alam, J., and Nath, K. A. (2007) Physiology and pathophysiology of heme: implications for kidney disease. *J. Am. Soc. Nephrol.* **18,** 414–420
18. Rajagopal, A., Rao, A. U., Amigo, J., Tian, M., Upadhyay, S. K., Hall, C., Uhm, S., Mathew, M. K., Fleming, M. D., Paw, B. H., Krause, M., and Hamza, I. (2008) Haem homeostasis is regulated by the conserved and concerted functions of HRG-1 proteins. *Nature* **453,** 1127–1231
19. Severance, S., Rajagopal, A., Rao, A. U., Cerqueira, G. C., Mitreva, M., El-Sayed, N. M., Krause, M., and Hamza, I. (2010) Genome-wide analysis reveals novel genes essential for heme homeostasis in *Caenorhabditis elegans*. *PLoS Genet.* **6,** e1001044
20. White, C., Yuan, X., Schmidt, P. J., Bresciani, E., Samuel, T. K., Campagna, D., Hall, C., Bishop, K., Calicchio, M. L., Lapierre, A., Ward, D. M., Liu, P., Fleming, M. D., and Hamza, I. (2013) HRG1 is essential for heme transport from the phagolysosome of macrophages during erythrophagocytosis. *Cell Metab.* **17,** 261–270
21. Chen, C., Samuel, T. K., Krause, M., Dailey, H. A., and Hamza, I. (2012) Heme utilization in the *Caenorhabditis elegans* hypodermal cells is facilitated by heme-responsive gene-2. *J. Biol. Chem.* **287,** 9601–9612
22. Huynh, C., Yuan, X., Miguel, D. C., Renberg, R. L., Protchenko, O., Philpott, C. C., Hamza, I., and Andrews, N. W. (2012) Heme uptake by *Leishmania amazonensis* is mediated by the transmembrane protein LHR1. *PLoS Pathog.* **8,** e1002795
23. Merli, M. L., Pagura, L., Hernández, J., Barisón, M. J., Pral, E. M., Silber, A. M., and Cricco, J. A. (2016) The *Trypanosoma cruzi* protein TcHTE is critical for heme uptake. *PLoS Negl. Trop. Dis.* **10,** e0004359
24. Renberg, R. L., Yuan, X., Samuel, T. K., Miguel, D. C., Hamza, I., Andrews, N. W., and Flannery, A. R. (2015) The heme transport capacity of LHR1 determines the extent of virulence in *Leishmania amazonensis*. *PLoS Negl. Trop. Dis.* **9,** e0003804
25. Cabello-Donayre, M., Malagarie-Cazenave, S., Campos-Salinas, J., Gálvez, F. J., Rodríguez-Martínez, A., Pineda-Molina, E., Orrego, L. M., Martínez-García, M., Sánchez-Cañete, M. P., Estévez, A. M., and Pérez-Victoria, J. M. (2016) Trypanosomatid parasites rescue heme from endocytosed hemoglobin through lysosomal HRG transporters. *Mol. Microbiol.* **101,** 895–908
26. Yuan, X., Protchenko, O., Philpott, C. C., and Hamza, I. (2012) Topologically conserved residues direct heme transport in HRG-1-related proteins. *J. Biol. Chem.* **287,** 4914–4924
27. Urbaniak, M. D., Martin, D. M., and Ferguson, M. A. (2013) Global quantitative SILAC phosphoproteomics reveals differential phosphorylation is widespread between the procyclic and bloodstream form lifecycle stages of *Trypanosoma brucei*. *J. Proteome Res.* **12,** 2233–2244
28. Siegel, T. N., Hekstra, D. R., Wang, X., Dewell, S., and Cross, G. A. (2010) Genome-wide analysis of mRNA abundance in two life-cycle stages of *Trypanosoma brucei* and identification of splicing and polyadenylation sites. *Nucleic Acids Res.* **38,** 4946–4957
29. Jensen, B. C., Ramasamy, G., Vasconcelos, E. J., Ingolia, N. T., Myler, P. J., and Parsons, M. (2014) Extensive stage-regulation of translation revealed by ribosome profiling of *Trypanosoma brucei*. *BMC Genomics* **15,** 911
30. Fadda, A., Ryten, M., Droll, D., Rojas, F., Färber, V., Haanstra, J. R., Merce, C., Bakker, B. M., Matthews, K., and Clayton, C. (2014) Transcriptome-wide analysis of trypanosome mRNA decay reveals complex degradation kinetics and suggests a role for co-transcriptional degradation in determining mRNA levels. *Mol. Microbiol.* **94,** 307–326
31. Telleria, E. L., Benoit, J. B., Zhao, X., Savage, A. F., Regmi, S., Alves e Silva, T. L., O'Neill, M., and Aksoy, S. (2014) Insights into the trypanosome-host interactions revealed through transcriptomic analysis of parasitized tsetse fly salivary glands. *PLoS Negl. Trop. Dis.* **8,** e2649
32. Alsford, S., Turner, D. J., Obado, S. O., Sanchez-Flores, A., Glover, L., Berriman, M., Hertz-Fowler, C., and Horn, D. (2011) High-throughput phenotyping using parallel sequencing of RNA interference targets in the African trypanosome. *Genome Res.* **21,** 915–924

33. Changmai, P., Horáková, E., Long, S., Černotíková-Stíbrná, E., McDonald, L. M., Bontempi, E. J., and Lukeš, J. (2013) Both human ferredoxins equally efficiently rescue ferredoxin deficiency in *Trypanosoma brucei*. *Mol. Microbiol.* **89,** 135–151
34. Dyer, N. A., Rose, C., Ejeh, N. O., and Acosta-Serrano, A. (2013) Flying tryps: survival and maturation of trypanosomes in tsetse flies. *Trends Parasitol.* **29,** 188–196
35. Houseman, J. G. (1980) Anterior midgut proteinase inhibitor from *Glossina morsitans morsitans* Westwood (Diptera: Glossinidae) and its effect upon tsetse digestive enzymes. *Can. J. Zool.* **58,** 79–87
36. Lehane, M. J. (2005) *The biology of blood-sucking insects*, 2nd Ed., pp. 82–91, Cambridge University Press, Cambridge, UK
37. Lara, F. A., Sant'anna, C., Lemos, D., Laranja, G. A., Coelho, M. G., Reis Salles, I., Michel, A., Oliveira, P. L., Cunha-E-Silva, N., Salmon, D., and Paes, M. C. (2007) Heme requirement and intracellular trafficking in *Trypanosoma cruzi* epimastigotes. *Biochem. Biophys. Res. Commun.* **355,** 16–22
38. Chang, K. P., Chang, C. S., and Sassa, S. (1975) Heme biosynthesis in bacterium-protozoon symbioses: enzymic defects in host hemoflagellates and complemental role of their intracellular symbiotes. *Proc. Natl. Acad. Sci. U.S.A.* **72,** 2979–2983
39. Kořený, L., Sobotka, R., Kovářová, J., Gnipová, A., Flegontov, P., Horváth, A., Oborník, M., Ayala, F. J., and Lukeš, J. (2012) Aerobic kinetoplastid flagellate *Phytomonas* does not require heme for viability. *Proc. Natl. Acad. Sci. U.S.A.* **109,** 3808–3813
40. Campos-Salinas, J., Cabello-Donayre, M., García-Hernández, R., Pérez-Victoria, I., Castanys, S., Gamarro, F., and Pérez-Victoria, J. M. (2011) A new ATP-binding cassette protein is involved in intracellular haem trafficking in *Leishmania*. *Mol. Microbiol.* **79,** 1430–1444
41. Halliwell, B., and Gutteridge, J. M. (1990) Role of free radicals and catalytic metal ions in human disease: an overview. *Methods Enzymol.* **186,** 1–85
42. Khan, A. A., and Quigley, J. G. (2011) Control of intracellular heme levels: heme transporters and heme oxygenases. *Biochim. Biophys. Acta* **1813,** 668–682
43. Natesan, S. K., Peacock, L., Matthews, K., Gibson, W., and Field, M. C. (2007) Activation of endocytosis as an adaptation to the mammalian host by trypanosomes. *Eukaryot. Cell* **6,** 2029–2037
44. Pal, J. K., and Joshi-Purandare, M. (2001) Dose-dependent differential effect of hemin on protein synthesis and cell proliferation in *Leishmania donovani* promastigotes cultured in vitro. *J. Biosci.* **26,** 225–231
45. Ciccarelli, A., Araujo, L., Batlle, A., and Lombardo, E. (2007) Effect of haemin on growth, protein content, and the antioxidant defense system in *Trypanosoma cruzi*. *Parasitology* **134,** 959–965
46. da Silva Augusto, L., Moretti, N. S., Ramos, T. C., de Jesus, T. C., Zhang, M., Castilho, B. A., and Schenkman, S. (2015) A membrane-bound eIF2α kinase located in endosomes is regulated by heme and controls differentiation and ROS levels in *Trypanosoma cruzi*. *PLoS Pathog.* **11,** e1004618
47. Rotureau, B., Subota, I., and Bastin, P. (2011) Molecular bases of cytoskeleton plasticity during the *Trypanosoma brucei* parasite cycle. *Cell. Microbiol.* **13,** 705–716
48. Sunter, J. D., Benz, C., Andre, J., Whipple, S., McKean, P. G., Gull, K., Ginger, M. L., and Lukeš, J. (2015) Modulation of flagellum attachment zone protein FLAM3 and regulation of the cell shape in *Trypanosoma brucei* life cycle transitions. *J. Cell Sci.* **128,** 3117–3130
49. Vassella, E., Oberle, M., Urwyler, S., Renggli, C. K., Studer, E., Hemphill, A., Fragoso, C., Bütikofer, P., Brun, R., and Roditi, I. (2009) Major surface glycoproteins of insect forms of *Trypanosoma brucei* are not essential for cyclical transmission by tsetse. *PLoS ONE* **4,** e4493
50. Knüsel, S., and Roditi, I. (2013) Insights into the regulation of GPEET procyclin during differentiation from early to late procyclic forms of *Trypanosoma brucei*. *Mol. Biochem. Parasitol.* **191,** 66–74
51. Vassella, E., Den Abbeele, J. V., Bütikofer, P., Renggli, C. K., Furger, A., Brun, R., and Roditi, I. (2000) A major surface glycoprotein of *Trypanosoma brucei* is expressed transiently during development and can be regulated post-transcriptionally by glycerol or hypoxia. *Genes Dev.* **14,** 615–626
52. Maric, D., Epting, C. L., and Engman, D. M. (2010) Composition and sensory function of the trypanosome flagellar membrane. *Curr. Opin. Microbiol.* **13,** 466–472
53. Hashimi, H., Zíková, A., Panigrahi, A. K., Stuart, K. D., and Lukeš, J. (2008) TbRGG1, an essential protein involved in kinetoplastid RNA metabolism that is associated with a novel multiprotein complex. *RNA* **14,** 970–980
54. Brenndörfer, M., and Boshart, M. (2010) Selection of reference genes for mRNA quantification in *Trypanosoma brucei*. *Mol. Biochem. Parasitol.* **172,** 52–55
55. Pfaffl, M. W. (2001) A new mathematical model for relative quantification in real-time RT-PCR. *Nucleic Acids Res.* **29,** e45
56. Vondrusková, E., van den Burg, J., Zíková, A., Ernst, N. L., Stuart, K., Benne, R., and Lukes, J. (2005) RNA interference analyses suggest a transcript-specific regulatory role for mitochondrial RNA-binding proteins MRP1 and MRP2 in RNA editing and other RNA processing in *Trypanosoma brucei*. *J. Biol. Chem.* **280,** 2429–2438
57. Dean, S., Sunter, J., Wheeler, R. J., Hodkinson, I., Gluenz, E., and Gull, K. (2015) A toolkit enabling efficient, scalable and reproducible gene tagging in trypanosomatids. *Open Biol.* **5,** 140197
58. Schiött, T., Throne-Holst, M., and Hederstedt, L. (1997) Bacillus subtilis CcdA-defective mutants are blocked in a late step of cytochrome *c* biogenesis. *J. Bacteriol.* **179,** 4523–4529

The *Trypanosoma brucei Tb*Hrg protein is a heme transporter involved in the regulation of stage-specific morphological transitions

Eva Horáková, Piya Changmai, Marie Vancová, Roman Sobotka, Jan Van Den Abbeele, Benoit Vanhollebeke and Julius Lukes

J. Biol. Chem. 2017, 292:6998-7010.
doi: 10.1074/jbc.M116.762997 originally published online February 23, 2017